Quantum Confinement in Monatomic Cu Chains on Cu(111)

S. Fölsch,[1,*] P. Hyldgaard,[2] R. Koch,[1] and K. H. Ploog[1]

[1]*Paul-Drude-Institut für Festkörperelektronik, Hausvogteiplatz 5-7, D-10117 Berlin, Germany*

[2]*Department of Applied Physics, Chalmers University of Technology and Göteborgs University, SE-41296, Göteborg, Sweden*

(Received 26 August 2003; published 5 February 2004)

The existence of one-dimensional (1D) electronic states in Cu/Cu(111) chains assembled by atomic manipulation is revealed by low-temperature scanning tunneling spectroscopy and density functional theory (DFT) calculations. Our experimental analysis of the chain-localized electron dynamics shows that the dispersion is fully described within a 1D tight-binding approach. DFT calculations confirm the confinement of unoccupied states to the chain in the relevant energy range, along with a significant extension of these states into the vacuum region.

DOI: 10.1103/PhysRevLett.92.056803 PACS numbers: 73.21.Hb, 68.37.Ef, 68.47.De, 71.15.Mb

Aside from the atomic-scale characterization of solid surfaces, low-temperature scanning tunneling microscopy (LT-STM) enables the manipulation of adsorbed atoms and molecules with atomic precision [1]. This combined approach makes LT-STM an ideal experimental tool to explore fundamental electronic processes in nanoscopic systems because it allows both to direct and to probe quantum confinement. This is of particular relevance to metallic nanostructures since here the Fermi wavelength is of the order of a few Å which demands confinement to atomic-scale dimensions in order to achieve quantization phenomena. The latter give rise to new physical behavior relevant to, e.g., catalytic [2], electronic [3,4], or magnetic properties [5]. Objects of special interest in terms of ultimate miniaturization are atomic chains serving as ''wires'' [6] which will play a leading role in future nanoscale electronics. Concepts were proposed to employ quasi-insulating templates to achieve electronic decoupling of such assembled structures [7]. Yet this approach encounters experimental difficulties since a definite degree of conductivity is required to execute STM measurements. Recently, Nilius *et al.* reported that monatomic Au chains on the alloy surface NiAl(110) [8] exhibit one-dimensional (1D) electronic states which suggests an appreciable degree of electronic decoupling from the metallic substrate. This finding was attributed to the pseudogap of the NiAl bulk bands projected along $\langle 110 \rangle$ [9].

In this Letter we demonstrate that the formation of quantized chain-localized states in the pseudogap of the substrate bulk band structure is a general phenomenon even observable for homogeneous metallic systems. We find that monatomic Cu/Cu(111) chains are characterized by remarkably distinct quantum levels. Compared to the electronic confinement in Au/NiAl(110) chains, the present system exhibits an increased ratio of energy separation to width of the observed levels. This permits us to clearly discern the respective eigenstates and to probe the on-chain electron dynamics in great detail. In contrast to a free-electron-like behavior proposed for Au/NiAl(110) chains [8], the 1D band dispersion observed here is fully described within a tight-binding approach accounting for the coupling between the atomic resonances associated with the chain atoms. Consistently, density functional theory (DFT) calculations reveal the existence of occupied as well as unoccupied chain-localized states and provide detailed insight into the accessibility of these states by STM probing. The present discovery of quantum wire behavior in a *homogeneous* metallic system is of direct practical importance since it avoids the electronic and structural complications inherent to heterogeneous systems. This opens up the possibility to explore phenomena of advanced complexity like, e.g., proximity effects between adjacent quantum structures or their electronic interaction with adsorbed molecules.

The experiments were carried out by LT-STM at a temperature of 7 K. The Cu(111) specimen was cleaned by standard procedures in ultrahigh vacuum (Ne sputtering at 1000 eV and annealing at 700 K). Single Cu adatoms were created by controlled tip-sample contact at 7 K. Monatomic Cu chains with the intrinsic nearest-neighbor spacing $a = 2.55$ Å were assembled by atomic manipulation along the close-packed row direction of the substrate at a tunneling resistance of ~ 0.1 MΩ. Figure 1 (right) shows constant-current images of a Cu monomer and a Cu dimer, and chains consisting of three, five, and seven atoms. The structural features observed here are in line with the recent work of Repp *et al.* [10], who showed that Cu_i ($i \geq 3$) clusters assembled by manipulation at 5–21 K are stable and preferably form monatomic chains with the Cu atoms residing on fcc sites. The Cu dimer, on the other hand, diffuses locally at temperatures >5 K within a cell of adjacent hcp and fcc sites centered around an on-top site [10]. The intracell diffusion is responsible for the unstable and round-shaped appearance of the Cu dimer in the STM image in Fig. 1. The left panel shows corresponding differential conductivity curves as a measure of the local density of states (LDOS) in the regime of unoccupied sample states. The spectrum of bare Cu(111) (bottom curve) indicates a virtually constant LDOS up

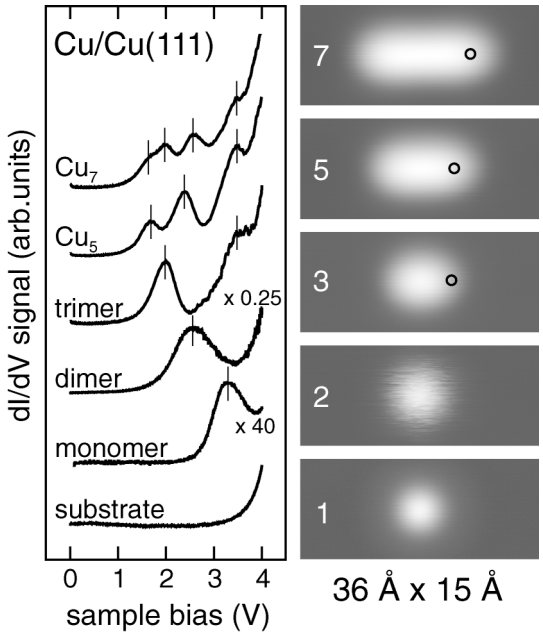

FIG. 1. Left: Differential conductivity dI/dV of bare Cu(111) in the regime of unoccupied sample states (bottom curve) and respective spectra measured over a Cu monomer, dimer, and monatomic Cu chains three, five, and seven atoms in length. All spectra taken at constant tip height with initial tunneling parameters of 1 nA and 1 V (equivalent to ~5.5 Å tip height) with the exception of the monomer spectrum, for which the tunneling current was reduced to 10 pA. Peaks marked by vertical bars indicate the formation of quantized states in the pseudogap of the projected Cu bulk band structure. The black circles in the corresponding STM images (right panel: 1 nA, 1 V, 7 K) mark the respective tip positions when taking dI/dV spectra; for the monomer and the dimer the tip was located over the center of the object.

to ~3.5 V and a steady increase at a higher sample bias which is attributed to the pseudogap of the projected Cu bulk band structure and the onset of image states below the vacuum level [11]. In contrast, when measuring the differential tunneling conductivity of a single Cu adatom a sharp peak in the LDOS is found slightly below 3.3 V with a full width at half maximum (FWHM) of ~0.6 V. This suggests that the Cu/Cu(111) monomer exhibits a pronounced quasiatomic resonance similar to the behavior reported for Pd monomers on Al_2O_3 layers [12] and single Au adatoms on NiAl(110) [8,13]. For the dimer we find a broadened peak (FWHM ~0.9 V) at a reduced sample bias of 2.6 V. With increasing chain length, the interatomic coupling yields a series of bound states whose energetic positions and separations decrease as the number of Cu atoms increases (in the case of a Cu_7 chain, for example, four states are observed in the investigated voltage range located at 1.7, 2.0, 2.6, and 3.5 V; cf. top curve of Fig. 1). Accordingly, the peak observed for the dimer at 2.6 V is attributed to the quasibonding ground state in analogy to the result found for Au dimers on NiAl(110) [13]. The peak broadening as well as the increased noise level in the dI/dV signal is a further indication of dimeric intracell diffusion at the present temperature of 7 K.

Figure 2 shows the square of the wave functions of the chain-localized states as determined from the spatial variation of the dI/dV signal at tunneling voltages where peaks in the LDOS are observed (cf. Fig. 1). In detail, the resulting dI/dV maps obtained for Cu_i chains with i equal to three, five, seven, and nine (cf. rows from top to bottom, left panel of Fig. 2) reveal clear symmetry properties of the corresponding eigenstates which are indicative of quantum confinement in a 1D potential well. Each column includes states of defined order n with $n = 1$ being the ground state with one single lobe and $(n - 1)$ specifying the number of nodes for states of higher order. Figure 2 (right) shows contours of the dI/dV signal measured along a Cu_{15} chain demonstraing that states with n lobes are accessible for orders as large as $n = 8$. Obviously, the chain ends induce an enhanced dI/dV signal at the outermost lobe positions. A similar observation has been reported for Au chains on NiAl(110) [8,14] and was attributed to two possible effects, namely, (i) the change in tip-sample separation while scanning over the chain edge with the feedback loop turned off [14], and (ii) the existence of zero-dimensional defect states localized at the chain ends [8].

To determine the dispersion of the 1D states observed here we extracted the characteristic wave length for $n = 3$ to $n = 8$ and chain lengths from five to 15 Cu atoms by evaluating nodal positions in the center region of the LDOS distributions. The effective width of the potential well $(n\lambda)/2$ estimated from the measured wave length fits within an error of $<4\%$ with the apparent chain length observed by constant-current imaging at identical tunneling parameters of 1 nA and 1 V. Figure 3 summarizes the energy-dependent wave vector values in quantities of π/a. It is revealed (i) that a uniform $E(k)$ dependence holds across the entire range of chain length investigated, and (ii) that the data are well fitted by the relation $E(k) = E_a - \beta - 2\gamma\cos(ka)$, implying a description of the problem by an effective 1D tight-binding Hamiltonian. Within this model the center of the resulting 1D band is located at $E_a - \beta = 3.1$ eV which is close to the resonance found for the monomer slightly below 3.3 eV (cf. Fig. 1). The value of the overlap integral $\gamma = 0.9$ eV, which is a measure for the coupling between the quasiatomic levels, yields a bandwidth of 3.6 eV. This value is equivalent to an effective electron mass of $m^* = \hbar^2/[\gamma 2a^2] = 0.68m_e$ at the band edges. To ensure that the observed $E(k)$ dispersion is not falsified by Stark shifts due to the tip electric field, we have monitored the energetic position of the ground state of the trimer centered at 2.0 V at tunneling currents from 20 pA to 0.2 μA; the resulting range in electric field is about 0.3–0.7 V/Å and includes typical fields at which dI/dV spectra like those in Fig. 1 were recorded. Within this range we find only a minor peak shift of ~20 mV. Hence,

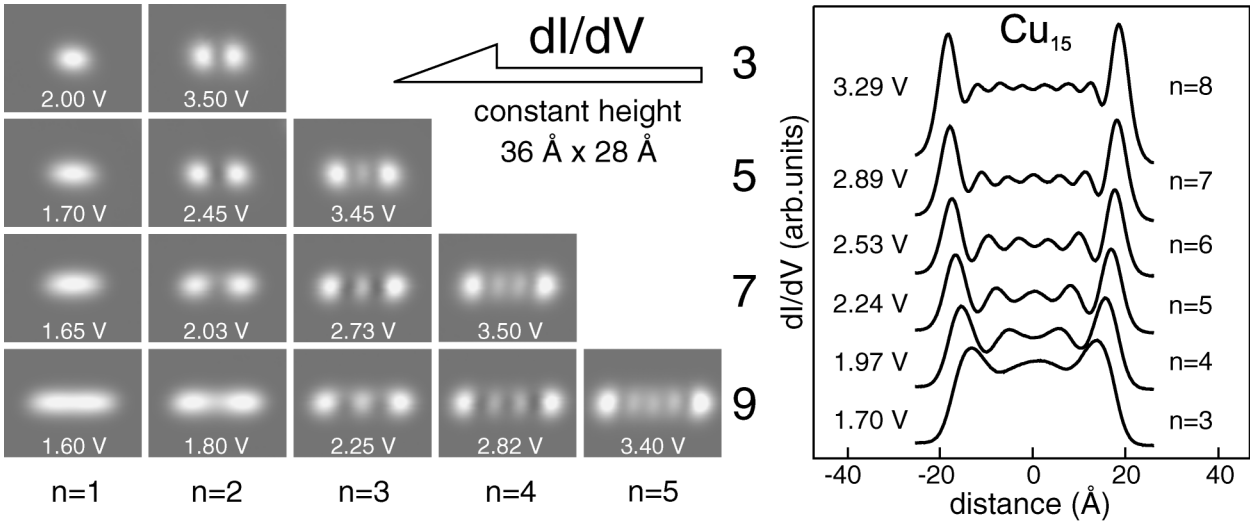

FIG. 2. Left panel: dI/dV maps measured at constant tip height showing the square of the wave function of the chain-localized states (tunneling parameters prior to opening the feedback loop: 1 nA, 1 V). Rows from top to bottom correspond to chains of three, five, seven, and nine atoms while columns include eigenstates of fixed order n (n: number of lobes). Right panel: dI/dV contours measured along a Cu_{15} chain for orders $n = 3$ to $n = 8$ taken at the same initial tunneling parameters as the dI/dV maps (left).

the relative energetic positions of the respective quantum levels which yield the dispersion in Fig. 3 are not affected to an appreciable extent.

To verify and complement our interpretation of the observed wave function localization we performed a number of DFT calculations [15] (cf. Fig. 4) using a five-layer slab with a three-by-one surface unit cell to represent the chain and the underlying surface. Band-structure calculations of the energetically favored fcc adatom chain configuration [10] served to identify three

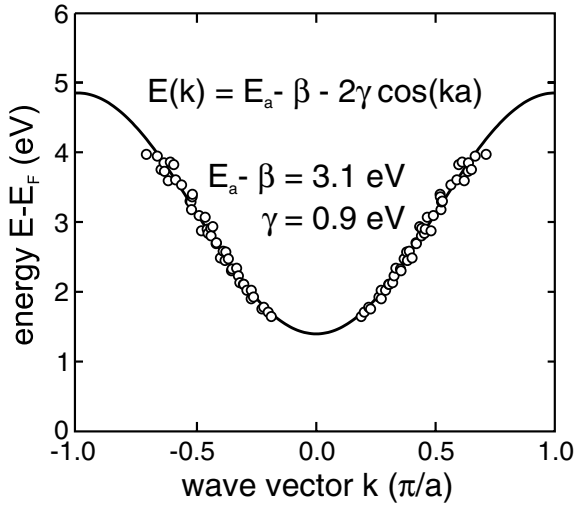

FIG. 3. The 1D band dispersion extracted from the characteristic wavelength for chain lengths from 5 to 15 atoms and $n = 3$ to $n = 8$, the wave vector is given in quantities of π/a ($a = 2.55$ Å is the Cu-Cu spacing). The experimental data are well fitted within the tight binding approximation yielding a band centered at 3.1 eV and an effective electron mass of $m^* = 0.68m_e$.

states trapped within the Cu(111) pseudogap showing vanishing dispersion except along the chains, which is indicative of an on-chain localization. Two of these states are occupied with the Γ point energy below the Fermi energy obtained from the self-consistent calculations. The third state is unoccupied and is characterized by a calculated Γ point energy of $E_0 = 0.9$ eV and an effective mass of $m^* = 0.71m_e$ (cf. $E_0 = 1.5$ eV and $m^* = 0.68m_e$ as experimental values extracted from the dispersion). We attribute the difference between the measured and the calculated E_0 value to the well-known difficulties of DFT to correctly predict the energy position of excited states like our unoccupied one-dimensional electron system. Figure 4 shows the wave function amplitude (contour sheets) and phase variation (coloring) of these three states relative to the atomic positions (red spheres) and verifies their on-chain or above-chain localization. Figure 4(a) details the spatial wave function variation of the unoccupied state — which is probed in the STM experiment — viewed along (left) and perpendicular to the chain direction (right). The panels show that this state has a simple phase variation and a significant extension into the vacuum region and therefore an enhanced accessibility for STM probing. The right panel in Fig. 4(a) adds an indication [16] (innermost contour) of the wave function core of the unoccupied state to justify the tight-binding approach used to interpret our experimental results. At the same time the DFT calculations reveal a surprising above-chain localization and a variation which is inconsistent with any pure s- or d-wave or even an s-d–hybrid nature. Instead, the calculations suggest that the STM-active state is formed by an along-chain linking of atomic orbitals that express also a significant amount of p_z-wave function character as will be discussed in detail in a forthcoming publication.

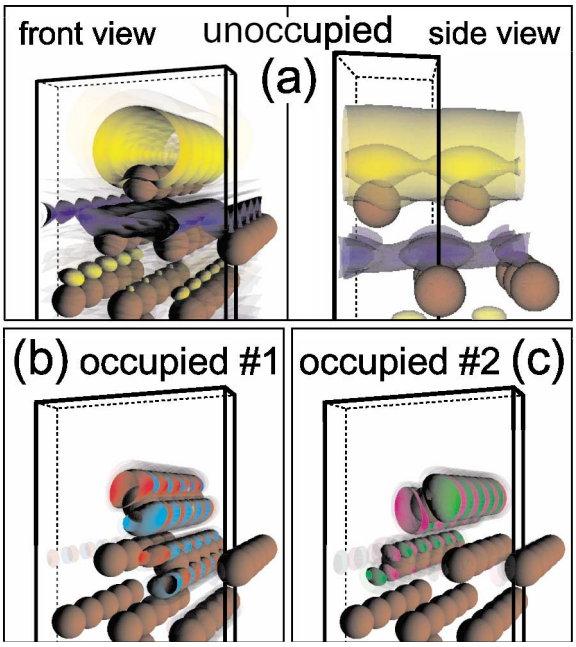

FIG. 4 (color). DFT-calculated wave functions of the unoccupied (a) and the two occupied chain-confined states (b) and (c), showing the wave function amplitude (contour sheets) and phase variation [blue-yellow (a), turquoise-red (b), and purple-green coloring (c)] relative to the atomic positions (red spheres) at wave vector $k = 0$. Black lines outline the unit cell containing the three-by-one five-layer slab used in the calculations. The unoccupied state (a) shows an appreciable extension into the vacuum region while the occupied d-like states (b) and (c) exhibit a stronger on-chain localization and a reduced coupling to the substrate.

Finally, Figs. 4(b) and 4(c) report our DFT-based prediction that the Cu(111) adatom chain formation also supports two occupied one-dimensional electron systems with a pronounced on-chain localization and almost pure d-wave nature. Both these states exhibit an even stronger quasi-1D confinement as compared to the unoccupied state. These states are more difficult to probe by STM due to their symmetry (the strong variation in wave function phase) and their lack of extension into the vacuum region. A comparison between the wave functions shown in 4(b) and 4(c) reveals subtle differences in the coupling to the underlying surface atoms, which explains a small energy splitting between the two occupied states. Thus, the DFT calculations corroborate essential experimental observations, namely, (i) the existence of 1D-confined quantum states trapped in the Cu(111) pseudogap, (ii) a significant extension of the unoccupied state into the vacuum region, and (iii) the central role of coupling between quasiatomic resonances in the formation of the chain-localized states.

In conclusion, the present results demonstrate that quantum confinement in surface-supported atomic-scale metal chains is a general phenomenon likely to be observable in numerous other metal-on-metal systems characterized by a pseudogap in the projected bulk band structure of the substrate. In that respect, the Cu(111) and noble-metal surface systems are superior in having a very large magnitude of the pseudogap. As documented both in the STM probing and by first-principle DFT calculations, the large pseudogap makes it possible to obtain well-resolved energy resonances and to examine the electron dynamics and intrinsic properties of these 1D quantum systems in unique detail. With regard to molecular electronics, it will be of utmost interest to study the interaction of these quantum wires with functional molecules in order to push forward the frontiers towards single molecule contacting and lateral networking on the atomic scale. In this context, quantum wires fabricated from homogeneous metallic systems provide a key advantage which will facilitate a detailed physical understanding even if the requirements become more complex.

This research was supported by the European Union projects NANOSPECTRA and ATOMCAD, and the Swedish foundation for strategic research, SSF.

*Corresponding author.
Electronic mail: foelsch@pdi-berlin.de

[1] See, e.g., D. M. Eigler and E. K. Schweizer, Nature (London) **344**, 524 (1990); G. Meyer, S. Zöphel, and K. H. Rieder, Phys. Rev. Lett. **77**, 2113 (1996).
[2] A. Sanchez *et al.*, J. Phys. Chem. A **103**, 9573 (1999).
[3] N. Nilius, N. Ernst, and H.-J. Freund, Phys. Rev. Lett. **84**, 3994 (2000).
[4] B. Razaznejad, C. Ruberto, P. Hyldgaard, and B. I. Lundqvist, Phys. Rev. Lett. **90**, 236803 (2003).
[5] M. Moseler, H. Häkkinen, R. N. Barnett, and U. Landman, Phys. Rev. Lett. **86**, 2545 (2001).
[6] J. Nogami, in *Atomic and Molecular Wires*, edited by C. Joachim and S. Roth (Kluwer, Dordrecht, 1997), Vol. 341, p. 11.
[7] T. Yamada, J. Vac. Sci. Technol. A **17**, 1463 (1999).
[8] N. Nilius, T. M. Wallis, and W. Ho, Science **297**, 1853 (2002).
[9] S.-C. Lui, M. H. Kang, E. J. Mele, E. W. Plummer, and D. M. Zehner, Phys. Rev. B **39**, 13149 (1989).
[10] J. Repp, G. Meyer, K. H. Rieder, and P. Hyldgaard, Phys. Rev. Lett. **91**, 206102 (2003).
[11] N. V. Smith, Phys. Rev. B **32**, 3549 (1985).
[12] N. Nilius, T. M. Wallis, and W. Ho, Phys. Rev. Lett. **90**, 046808 (2003).
[13] N. Nilius, T. M. Wallis, M. Persson, and W. Ho, Phys. Rev. Lett. **90**, 196103 (2003).
[14] T. M. Wallis, N. Nilius, and W. Ho, Phys. Rev. Lett. **89**, 236802 (2002).
[15] We used the DACAPO (http://www.fysik.dtu.dk/CAMPOS) ultrasoft plane-wave code in the generalized gradient approximation (PW91) and with dipole correction enabled, a 4-by-12 k-point sampling, and a 30 Ry energy cutoff.
[16] Being based on a pseudopotential approach, our DFT calculations are approximate only in the determination of the wave function core.